Supporting Information

Gendre et al. 10.1073/pnas.1018371108

SI Materials and Methods

Plant Material. The *ech* T-DNA insertion mutant line (SAIL_163_E09, Col0, Basta^R) was obtained from the Salk Institute. The transgenic fluorescent-protein marker lines in Col-0 background used were as follows: *pRAB-A2a::YFP-RABA2a* (1), p35*S::GFP-SYP41* (2), *pSYP61::SYP61-CFP* (3), *pARF1::ARF1-GFP* (4), *HS::BRI1-YFP* (5), p35*S::sec-GFP S76* (6), *pARA6::ARA6-GFP* (7), *pVHA-a1::VHA-a1-GFP* (8), *p35S::N-ST-YFP*, and *p35S::NAG1-EGFP* (9) and in Ws background: p35S::Aleu-GFP (10).

Plants were grown in soil (16 h light/8 h dark; 24 °C/19 °C; 150 uE/m^2 per s; 70% humidity) or in vitro on 2.2 g/L Murashige & Skoog nutrient mix (Duchefa), 0.7% plant agar (Duchefa), 0.5% sucrose, buffered to pH 5.8 with Mes (2-Morpholinoethanesulfonic acid; Sigma), after 2 d of vernalization. For experiments with dark-grown seedlings, seedlings were grown without sugar and with 5-h light treatment preceding 4 d incubation in the dark on plates wrapped in aluminum foil. Seeds were surface sterilized in 70% ethanol, 0.1% Tween 20 (vol/vol) for 5 min and rinsed in 99.5% ethanol. Concanamycine A (Sigma-Aldrich) treatment was performed as described (11).

For double mutant analysis, fluorescent markers were screened using an epifluorescence microscope and selected for the *ech* phenotype. Final molecular genotyping was performed to verify *ech* homozygote plants by using the primers Ech_RX2 GGTTTAACATTTGTCCAATG, Ech_FX2 ATATTATTGGGCCAGAGAAG; QRB1 TTCTGATAATGGGTGGTACTCGA in FX2-RX2 and QRB1-RX2 combinations.

Bioinformatic Analysis for Selection of *ECHIDNA* for Functional Analysis. Data from microarray experiments describing gene expression patterns across the wood-forming zone of *Populus. tremula* × *P. tremuloides* (12) was used, and 150 transcripts with a peak expression in the expanding secondary xylem were identified (12). Among those genes, 15 had a single ortholog in *Arabidopsis* and were selected for further analysis. The expression of these 15 genes was investigated in the various tissues and cell types and developmental stages of *Arabidopsis* by using Genevestigator (13) as well as in microarray datasets describing gene expression across the different developing zones of the *Arabidopsis* roots covering meristematic cells to fully elongated cells (14). *ECHIDNA* expression was found to be consistently higher in all datasets, in tissues and cell types undergoing elongation and expansion in *Arabidopsis*, e.g., root elongation zone hypocotyls, and was therefore selected for functional analysis.

Root, Hypocotyl and Cell Length Measurement. Root cells lengths were measured on fully elongated epidermal cells on the upper third of the root and hypocotyl cells lengths were measured on fully elongated cells between the 6th and 10th cells from the bottom (15), using an Axioplan 2 microscope equipped with differential-interference-contrast optics (Zeiss), an Axiocam (Zeiss), and Axiovision software (Zeiss). Five cells from 10 individuals were measured for each experiment (two repeats). Graphs represent the average and the SD from three independent experiments.

Root and hypocotyl lengths were measured with Image J (16) on pictures taken at full resolution with a Canon 350D camera. Twenty to thirty individuals are measured for each experiment, and the experiment is done three times. Graphs represent the average and the SD of the three experiments.

A Student's *t* test was used to test for significance of difference between distributions of root and hypocotyl lengths in WT and *ech*.

Plasmid Construction and Plant Transformation. *ECH* promoter (2.4 kb) was amplified with 5′-AscI, GGGGGCGCGCCATAACAATGAGTTTTCTGAACA and 3′-PacI, GGGGGTTAATTAACTTTCGAAGAATCCAAAAGG and *ECH* genomic sequence was amplified with 5′-PacI, GGGGGTTAATTAAATGGACCCTAATAATCAGGTG and 3′-SpeI, GGGACTAGTGACAAGGGTGAAGGCAGATTGTACTG. After digestion, both fragments were ligated into AscI- and SpeI-digested vector pSL34 carrying EYFP in frame (17). *Arabidopsis* Col-0 ecotype was used for plant transformation by floral dip method (18).

Confocal Laser-Scanning Microscopy, Immunostaining, FM4-64 Staining and Inhibitor Treatments. Whole-mount immunolabeling as well as fluorescence detection by confocal laser-scanning microscopy (CLSM) was performed by using a Leica TCS SP2 AOBS (Leica) spectral CLSM system mounted on an LEICA DM IRE2 inverted microscope as described (19). In multilabeling studies, detection was in sequential line-scanning mode with a line average of 8. Antibodies dilutions were rabbit anti-ECH (1:600), rabbit anti-SYP21 (1:500) (20), rabbit anti-ELP (1:500) (21), rabbit anti-RAB-F2b (1:200) (22), rabbit anti-RAB-A2a (1:6,000) (kindly provided by I. Moore, University of Oxford), guinea pig anti-PIN2 (1:1,000) (23) and mouse anti-BIP/Hsc70 (Stressgen Bioregeant). Secondary antibody was Cy5-coupled donkey anti-rabbit IgG (1:300), TRITC-coupled donkey anti-guinea pig (1:125), and TRITC-coupled donkey anti-mouse (1:150) (Jackson ImmunoResearch). FM4-64 (Molecular Probes) staining was performed as described in ref. 24. Inhibitor treatment was carried out as described by using 50 μM BFA (Sigma) for 1 h (24) and 10 μM ConcA (Sigma) for 1 h (8).

Quantitative Analysis of Colocalization. Colocalization was performed assessing the proximity of the geometric centers (centroids) of objects in two different channels within the objective resolution (25). The centroid coordinates were obtained by using 3D objects counter in Image J (26). Four to six cells from each of 10 individual roots were analyzed for quantification.

Yeast Complementation. Yeast mutant strains (27) were grown in YEPD at 23 °C (1% bacto-yeast extract; 2% bacto-peptone and 2% glucose), transformed (28) with the pDR195 empty vector or expressing ECH from *ECH* cDNA, and plated on selective medium (dropout minus Ura; US Biological). After an overnight culture from a single fresh colony, the OD_{600} values of all cultures were adjusted to the same value and then diluted in 10-fold dilution steps with medium. Drops of medium at the different dilutions were applied to an SD-Ura dropout medium plate, and plates were incubated for 2 d at 22 or 35 °C.

Southern and Western Blot. Genomic DNA from WT and *ech* rosette was prepared by using Dneasy plant maxi-kit (Qiagen). Samples (2 μg) of DNA were digested with HindIII and size-fractioned by electrophoresis in 1.0% (wt/vol) agarose gel. Southern blot was realized according to standard protocol (29). The ^{32}P-labeled probe for hybridization was synthesized by Random Primed StripAble DNA Probe Synthesis and Removal Kit (Ambion) from a dsDNA template (PCR-amplified from WT cDNA by using primers X5′Bam, GGGGGATCCAATAAGGTGTTTCGTTTCTGCT and xXho1, GGGCTCGAGTCTTTGTACACCGTCTTTGCTCTCACA. Image analysis was realized by using a phosphorimager.

For Western blot, proteins were extracted according to ref. 30 with the following modifications: 2 mM DTT in the extraction

buffer. Proteins were further quantified with the DC protein assay kit from Bio-Rad. Thirty micrograms of total proteins were used to load a 12% acrylamide gel. ECH (1:100) and CDK-A (1:4,000) followed by anti-rabbit coupled with HRP (1:4,000) and anti-mouse HRP (1:3,000) antibodies were used for ECH and CDK specific detection, respectively.

Transmission Electron Microscopy. High pressure freezing of 7-d-old root tips was done by using a Leica EM HPM100. A 15% Dextran solution was used as extracellular cryoprotectant, and samples were frozen in Ted Pella "B" hats (Ted Pella). Freeze substitution was carried out with 2% osmium tetroxide and 8% dimethoxypropane in anhydrous acetone for 5 d. During this process, the cryovials were kept at −78 °C in an acetone-filled beaker packed in a styrofoam insulation box. This process was followed by infiltration and embedding in Spurr's epoxy resin. Ultrathin (70 nm) sections were prepared and picked up on formvar-coated grids. The grids were stained with 2% uranyl acetate in 70% methanol and Reynolds' lead citrate for 12 and 6 min, respectively. Samples were viewed on a Hitachi H7600 PC-TEM (Hitachi) at an accelerating voltage of 80 kV, and images recorded with an ATM Advantage HR digital CCD camera (Advanced Microscopy Techniques). Two separate sets of samples were independently high pressure frozen, embedded, and viewed for TEM.

Phylogenetic Analysis. Related proteins from yeast, human, and other plant species were aligned by using the program ClustalX version 1.8. Based on conserved regions (67 residues), a phylogenetic analysis was performed with the PROTDIST and NEIGHBOR programs of the PHYLIP 3.2 package (31). A phylogenetic tree was then inferred by the neighbor-joining method (32), tested with 1,000 replications in the bootstrap analysis, carried out with the SEQBOOT and CONSENSE programs in the same package, and visualized by using the TREEVIEW program (33).

1. Chow CM, Neto H, Foucart C, Moore I (2008) Rab-A2 and Rab-A3 GTPases define a trans-golgi endosomal membrane domain in Arabidopsis that contributes substantially to the cell plate. *Plant Cell* 20:101–123.
2. Uemura T, et al. (2004) Systematic analysis of SNARE molecules in Arabidopsis: Dissection of the post-Golgi network in plant cells. *Cell Struct Funct* 29:49–65.
3. Robert S, et al. (2008) Endosidin1 defines a compartment involved in endocytosis of the brassinosteroid receptor BRI1 and the auxin transporters PIN2 and AUX1. *Proc Natl Acad Sci USA* 105:8464–8469.
4. Xu J, Scheres B (2005) Dissection of Arabidopsis ADP-RIBOSYLATION FACTOR 1 function in epidermal cell polarity. *Plant Cell* 17:525–536.
5. Geldner N, Hyman DL, Wang X, Schumacher K, Chory J (2007) Endosomal signaling of plant steroid receptor kinase BRI1. *Genes Dev* 21:1598–1602.
6. Zheng H, Kunst L, Hawes C, Moore I (2004) A GFP-based assay reveals a role for RHD3 in transport between the endoplasmic reticulum and Golgi apparatus. *Plant J* 37: 398–414.
7. Goh T, et al. (2007) VPS9a, the common activator for two distinct types of Rab5 GTPases, is essential for the development of Arabidopsis thaliana. *Plant Cell* 19: 3504–3515.
8. Dettmer J, Hong-Hermesdorf A, Stierhof YD, Schumacher K (2006) Vacuolar H+-ATPase activity is required for endocytic and secretory trafficking in Arabidopsis. *Plant Cell* 18:715–730.
9. Grebe M, et al. (2003) Arabidopsis sterol endocytosis involves actin-mediated trafficking via ARA6-positive early endosomes. *Curr Biol* 13:1378–1387.
10. Di Sansebastiano GP, Paris N, Marc-Martin S, Neuhaus JM (2001) Regeneration of a lytic central vacuole and of neutral peripheral vacuoles can be visualized by green fluorescent proteins targeted to either type of vacuoles. *Plant Physiol* 126:78–86.
11. von der Fecht-Bartenbach J, et al. (2007) Function of the anion transporter AtCLC-d in the trans-Golgi network. *Plant J* 50:466–474.
12. Hertzberg M, et al. (2001) A transcriptional roadmap to wood formation. *Proc Natl Acad Sci USA* 98:14732–14737.
13. Zimmermann P, Hirsch-Hoffmann M, Hennig L, Gruissem W (2004) GENEVESTIGATOR. Arabidopsis microarray database and analysis toolbox. *Plant Physiol* 136:2621–2632.
14. De Rybel B, et al. (2010) A novel aux/IAA28 signaling cascade activates GATA23-dependent specification of lateral root founder cell identity. *Curr Biol* 20:1697–1706.
15. Gendreau E, et al. (1997) Cellular basis of hypocotyl growth in Arabidopsis thaliana. *Plant Physiol* 114:295–305.
16. Abramoff MD, Magelhaes PJ, Ram SJ (2004) Image Processing with ImageJ. *Biophotonics International* 11:36–42.
17. Ikeda Y, et al. (2009) Local auxin biosynthesis modulates gradient-directed planar polarity in Arabidopsis. *Nat Cell Biol* 11:731–738.
18. Clough SJ, Bent AF (1998) Floral dip: A simplified method for Agrobacterium-mediated transformation of Arabidopsis thaliana. *Plant J* 16:735–743.
19. Fischer U, et al. (2006) Vectorial information for Arabidopsis planar polarity is mediated by combined AUX1, EIN2, and GNOM activity. *Curr Biol* 16:2143–2149.
20. Sanderfoot AA, et al. (1998) A putative vacuolar cargo receptor partially colocalizes with AtPEP12p on a prevacuolar compartment in Arabidopsis roots. *Proc Natl Acad Sci USA* 95:9920–9925.
21. Ahmed SU, Bar-Peled M, Raikhel NV (1997) Cloning and subcellular location of an Arabidopsis receptor-like protein that shares common features with protein-sorting receptors of eukaryotic cells. *Plant Physiol* 114:325–336.
22. Ueda T, Yamaguchi M, Uchimiya H, Nakano A (2001) Ara6, a plant-unique novel type Rab GTPase, functions in the endocytic pathway of Arabidopsis thaliana. *EMBO J* 20: 4730–4741.
23. Tromas A, et al. (2009) The AUXIN BINDING PROTEIN 1 is required for differential auxin responses mediating root growth. *PLoS ONE* 4:e6648.
24. Boutté Y, et al. (2010) Endocytosis restricts Arabidopsis KNOLLE syntaxin to the cell division plane during late cytokinesis. *EMBO J* 29:546–558.
25. Boutté Y, Crosnier MT, Carraro N, Traas J, Satiat-Jeunemaitre B (2006) The plasma membrane recycling pathway and cell polarity in plants: Studies on PIN proteins. *J Cell Sci* 119:1255–1265.
26. Bolte S, Cordelières FP (2006) A guided tour into subcellular colocalization analysis in light microscopy. *J Microsc* 224:213–232.
27. Inadome H, Noda Y, Kamimura Y, Adachi H, Yoda K (2007) Tvp38, Tvp23, Tvp18 and Tvp15: Novel membrane proteins in the Tlg2-containing Golgi/endosome compartments of Saccharomyces cerevisiae. *Exp Cell Res* 313:688–697.
28. Dohmen RJ, Strasser AW, Höner CB, Hollenberg CP (1991) An efficient transformation procedure enabling long-term storage of competent cells of various yeast genera. *Yeast* 7:691–692.
29. Sambrook J, Russell D (2006) *The Condensed Protocols From Molecular Cloning: A Laboratory Manual* (Cold Spring Harbor Lab Press, Plainview, NY), p 800.
30. Gama F, et al. (2007) The mitochondrial type II peroxiredoxin from poplar. *Physiol Plant* 129:196–206.
31. Felsenstein J (1988) Phylogenies from molecular sequences: Inference and reliability. *Annu Rev Genet* 22:521–565.
32. Saitou N, Nei M (1987) The neighbor-joining method: A new method for reconstructing phylogenetic trees. *Mol Biol Evol* 4:406–425.
33. Page RD (1996) TreeView: an application to display phylogenetic trees on personal computers. *Comput Appl Biosci* 12:357–358.

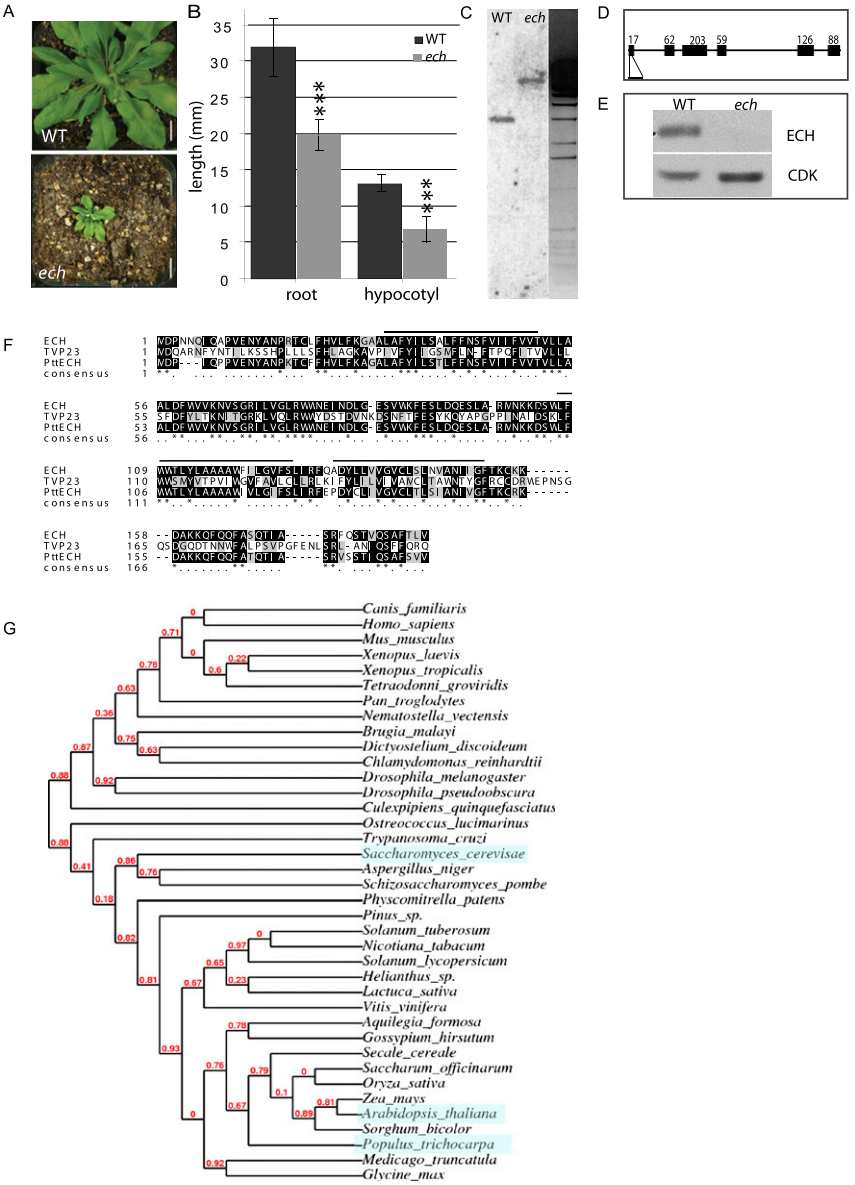

Fig. S1. Complementary analysis of *ech* phenotype, genetics, and phylogeny. (*A*) WT and *ech* mature leaves (26 d old). Note the size difference. (*B*) Average root length of 11-d-old seedlings and hypocotyl length of 4-d-old dark-grown seedlings. Measurements are an average (±SD) of three biological replicates, each of 100 seedlings. Significant differences are indicated as $*P < 0.01$ and $**P < 0{,}001$. (*C*) Southern blot performed on HindIII-digested genomic DNA from WT (line 1) and the homozygous *ech* mutant (line 2) with ^{32}P-labeled *ECH* cDNA as probe. (*D*) Exons/introns positions in the *ECH* gene (from TAIR prediction) and T-DNA insertion position in the promoter. (*E*) Western blot analysis of ECH expression in WT and *ech* total protein extracts (20 μg). CDK-A expression is used as loading control. (*F*) Multiple proteins sequence alignment of ECH, TVP23, and PttECH conducted with T-coffee (http://tcoffee.vital-it.ch/cgi-bin/Tcoffee/tcoffee_cgi/index.cgi) and the shading with Boxshade. Identical residues are indicated in black and are asterisked when identical across all three organisms. In gray are the positives matches. Above lines represent the consensus transmembrane domains (http://aramemnon.botanik.uni-koeln.de). (*G*) Phylogenetic tree with ECH orthologs in several plants (dicot and monocot), yeast, animal, and unicellular organisms. Accessions numbers are as follows: *Physcomitrella patens* (XP_001769534); *Ostreococcus lucimarinus* (XP_001417361); *Trypanosoma cruzi* (XP_810596.1); *Schizosaccharomyces pombe* (NP_596214); *Drosophila pseudoobscura* (XP_001353721.1); *Dictyostelium discoideum* (XP_643212.1AX4); *Nematostella vectensis* (XP_001630087.1); *Culexpipiens quinquefasciatus* (XP_001866515.1); *Drosophila melanogaster* (AAL48919.1); *Aspergillus niger* (XP_001389284.1); *Canis familiaris* (XP_546636.2); *Xenopus laevis* (AAH87467.1); *Brugia malayi* (XP_001900848.1); *Tetraodonni groviridis* (CAG03045.1); *Pan troglodytes* (XP_511818.2); *Xenopus tropicalis* (NP_001005091.1); *Homo sapiens* (NP_057162.4); *Chlamydomonas reinhardtii* (XP_001692072.1); *Mus musculus* (NP_080486.1); *Saccharomyces cerevisae* (Ydr084c); *Gossypium hirsutum* (cotton; TC32761); *Aquilegia formosa* (TC14924); *Medicago truncatula* (TC101774); *Glycine max* (soybean, TC206532); *Helianthus sp.* (Sunflower TC16516); *Vitis vinifera* (Grape; TC55687); *Lactuca sativa* (Lettuce; TC9607); *Nicotiana tabacum* (Tobacco;TC4656); *Solanum lycopersicum* (Tomato; TC179927); *Zea mays* (Maize; TC331451); *Saccharum officinarum* (Sugarcane; TC66487); *Oryza sativa* (Rice;TC296211); *Arabidopsis thaliana* (At1g09330); *Populus trichocarpa* (TC44460); *Sorghum bicolor* (TC106414); *Solanum tuberosum* (Potato; TC150216); *Pinus sp.* (TC74567); *Secale cereale* (Rye; TC3604).

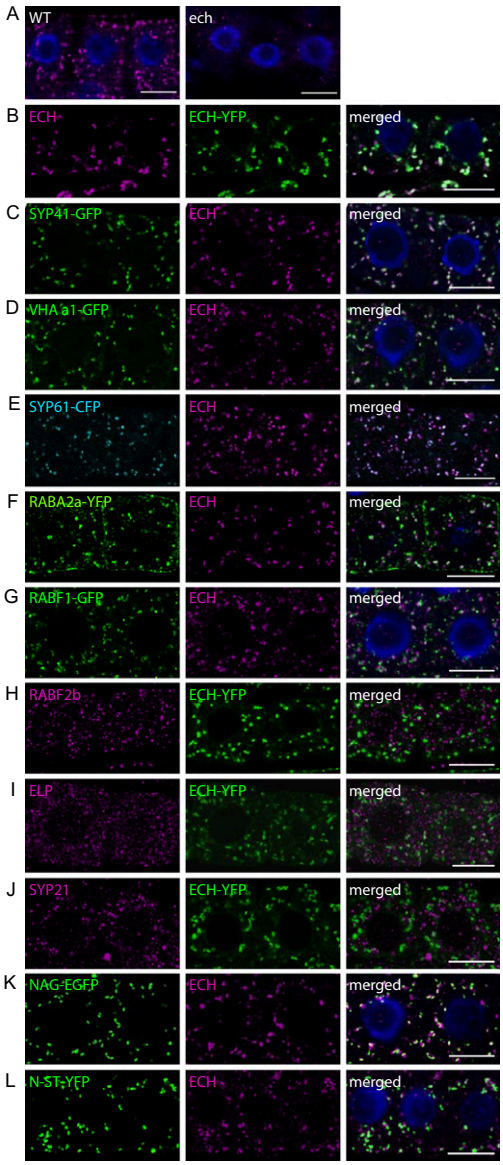

Fig. S2. ECH colocalized preferentially with TGN proteins. (*A*–*H*) Whole-mount immunostaining of root tips (5-d-old *Arabidopsis* seedling). (*A*) ECH antibody specificity (1:600) on WT and *ech* seedlings. (*B*) Colocalization of ECH immunolabeled signal (magenta) with ECH-YFP–labeled signal (green). (*C*–*H*) Representative confocal images of colocalization between ECH (*Center*) and various markers (*Left*). Either ECH-YFP (green; *Center*) or ECH antibody (magenta; *Center*) were used together with the following markers: SYP41-GFP (*C*), VHA-a1-GFP (*D*), SYP61-CFP (*E*), RABA2a-YFP (*F*), RABF1-GFP (*G*), RABF2b antibody (*H*), ELP antibody (*I*), SYP21 antibody (*J*), NAG-EGFP (*K*), and *N*-ST-YFP (*L*). (Scale bars: 10 μm.)

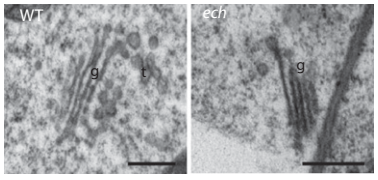

Fig. S3. *ech* has smaller Golgi bodies and less association between Golgi and TGN. Transmission electron micrographs of Golgi from WT showing an associated TGN and from *ech* showing absence of a TGN. Note the difference of Golgi size. g = Golgi, t = TGN. (Scale bars: 500 nm.)

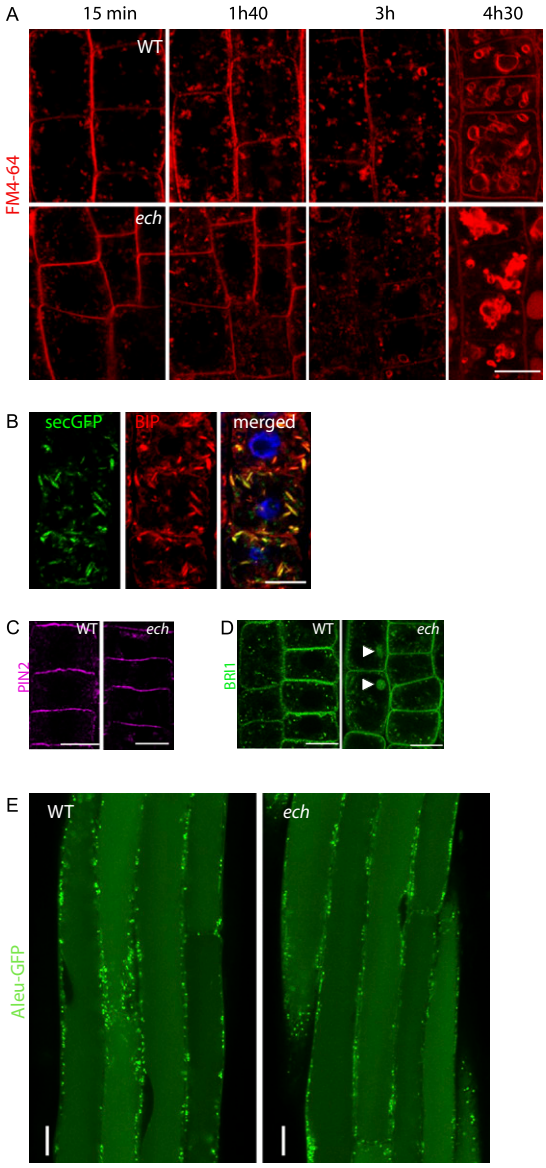

Fig. S4. Neither endocytosis nor vacuolar traffic is affected in *ech* but secretion is. (*A*) Time course of FM4-64 internalization in root epidermal cells, from 15 min to 4 h 30 min after FM4-64 labeling, of WT (*Upper*) and *ech* (*Lower*) seedlings. (*B*) Whole-mount immunostaining of 5-d-old *ech* expressing secGFP (green) with anti-BIP (red), an ER marker. *Right* represents the merged picture. (*C*) Anti-PIN2 immunolabeling of WT and *ech* root epidermal cells. (*D*) BRI1-YFP localization in WT and *ech* live root cells after 1 h of heat-shock treatment and 30 min recovery from heat shock. Abnormal vacuolar staining is shown by arrowheads. (*E*) Aleu-GFP fluorescent pattern in elongated root cells of WT and *ech* mutant. Aleu-GFP accumulates in the large central vacuole as well as in not-yet-identified punctate structures in both genotypes. (Scale bars: 10 μm.)

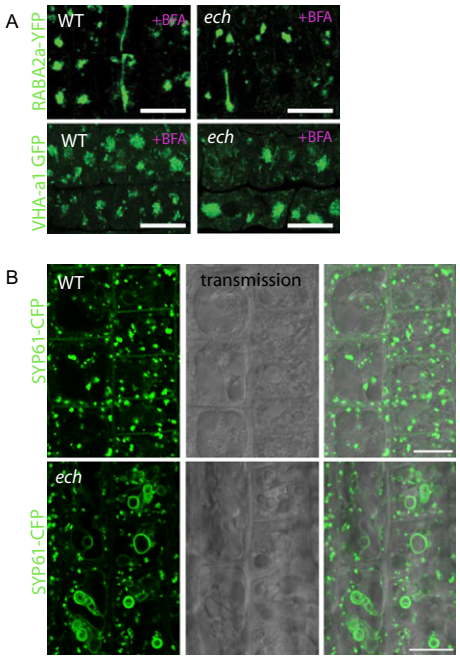

Fig. S5. RABA2a and VHA-a1 are still responding to BFA and SYP61 is also mislocalized at the tonoplast in *ech*. Confocal microscopy images from live root epidermal cells of WT and *ech* expressing RABA2a-YFP (*A, Upper*), VHA-a1-GFP (*A, Lower*) or SYP61-CFP (*B*), all under control of their own promoter. In *A*, seedlings are treated 1 h with 50 μM BFA. (Scale bars: 10 μm.)